Contribution to the Development of HVDC Circuit Breaker Technologies: A Review of New Considerations

Zhou Liu, Seyed Sattar Mirhosseini, Lian Liu, Marjan Popov, Kaiqi Ma, Weihao Hu, Sadegh Jamali, Peter Palensky, Zhe Chen

Abstract: In order to promote the integration of renewable energy resources in modern energy systems, HVDC and circuit breaker technologies become critical to achieve the secure and efficient energy transmission. This paper reviews the technical development of the related areas, compares diverse breaker concepts and topologies, investigates possible coordination and testing solutions, and points out the remaining challenges as well as future needs. The time domain simulation and comparative analysis are adopted in this paper to analyse and compare the performances of different HVDC circuit breakers. By making use of different selectivity levels of multi-terminal HVDC grids, the suitable planning and placement of HVDC circuit breakers can be conducted. Furthermore, by providing insights in the performance of HVDC circuit breakers, the work presented in this paper can serve as a useful asset for the upcoming standardization and industrial application process of HVDC grid and circuit breaker design and testing.

Index Terms — HVDC circuit breaker, comparative performance analysis, cost analysis based planning, synthetic testing, multi-terminal HVDC grid.

List of abbreviations

HVDC	High voltage direct current
MTDC	Multi-terminal HVDC
DC CB	Direct current circuit breaker
AC CB	Alternating current circuit breaker
LCC	Line commutated converter
VSC	Voltage source converter
MMC	Modular multi-level converter
TIV	Transient interruption voltage
MCB	Mechanical circuit breaker
SSCB	Solid-state circuit breaker
HCB	Hybrid circuit breaker
LCS	Load current switch

MB	Main breaker
UFD	Ultra-fast disconnector
SA	Surge arrester
MP HCB	Multi-port HCB
IMB	Integrated main breaker
ILCS	Integrated load current switch
RCB	Residual circuit breaker
VARCCB	VSC assisted resonant current circuit breaker
VI	Vacuum interrupter
FCS	Fault clearing strategy
TSG	Triggered spark gap

1. Introduction

Nowadays, it becomes a general trend in power systems to exploit the renewable energy resources instead of traditional fossil fuels, since they have more advantages related to environment and inexhaustible energy cycle [1]. In order to help integrating and transferring a large amount of the renewable energy resources, especially from diverse onshore and offshore sites, the development of MTDC grid becomes an emerging demand. Some relevant leading projects have been commissioned or being developed, e.g. Quebec-New England 3-terminal HVDC system [2], Nan'ao 4-terminal HVDC system [3] and Zhou Shan 5-terminal grids [4].

The main challenge when implementing MTDC grids is the vulnerability of such grids resulting from DC short circuit faults [5]. Due to the fast DC current rise, the outages caused by such severe disturbances can easily propagate from one to another converter station. Thus, the DC CB is of a vital importance to make the MTDC grid secure and to pave the way toward integration of bulk amount of offshore wind power to AC grid, in order to ensure system's high efficiency, reliability, and controllability [6] [7]. Until now, DC CBs are widely available for the application in the medium and low DC voltage levels [8]. Because of high requirements on fault detection, fault current interruption and energy dissipation in HVDC system, the most important challenges to realize MTDC grids are DC CBs and DC protection.

The timeline for the development of DC CBs is shown in Fig.1. As we know, Thomas Edison is regarded as an originator on the development of the DC power system, and the DC technology could have existed even earlier [10]. Along with the development of HVDC systems, the research on DC CB commenced in 1940s, which was earlier than the commissioning of the first commercial HVDC transmission link in 1954 [11]. From 1940s to 1980s, LCC HVDC systems evolved from mercury arc valve-based HVDC to thyristor-based ones (born in 1970s); and with a high interest in multi-terminal HVDC grid in 1980s, a lot of research on DC CB was conducted subsequently [12]. As one of the most important achievements, Hitachi successfully tested a 250 kV/8 kA mechanical HVDC CB in 1985 [13]. In 1988, another mechanical HVDC CB with the rating of 500 kV/4 kA was tested by BBC, EPRI and BPA [14]. Although, as seen in Fig. 1, the interest in HVDC CB declined after 1988, it arose again by emerging VSC HVDC systems resulting from the development of VSC and MMC in 1997 and 2003, respectively [15] [16]. The fault-interrupting speed of the breakers used in LCC HVDC systems is much lower than the minimum requirement of VSC HVDC systems. In 2011, the successful testing of 320 kV/16 kA ABB hybrid HVDC CB was performed [17]. A 200 kV/15 kA hybrid DC CB consisting of cascaded full-bridge IGBT submodules has been installed in Zhoushan MTDC grid [18] in 2016, and a 500 kV hybrid DC CB with the similar structure is going to be deployed in Zhangbei MTDC grid. In 2018, the world's first 160 kV/9 kA mechanical HVDC CB was utilized in the China southern power grid (CSG)'s Nan'ao MTDC grid [9]. The 160 kV/16 kA Mitsubishi Electric mechanical HVDC CB was successfully tested in 2019 [19]. In 2020, successful testing was performed on 80 kV/15 kA SCiBreak VSC assisted resonant current HVDC CB [20].

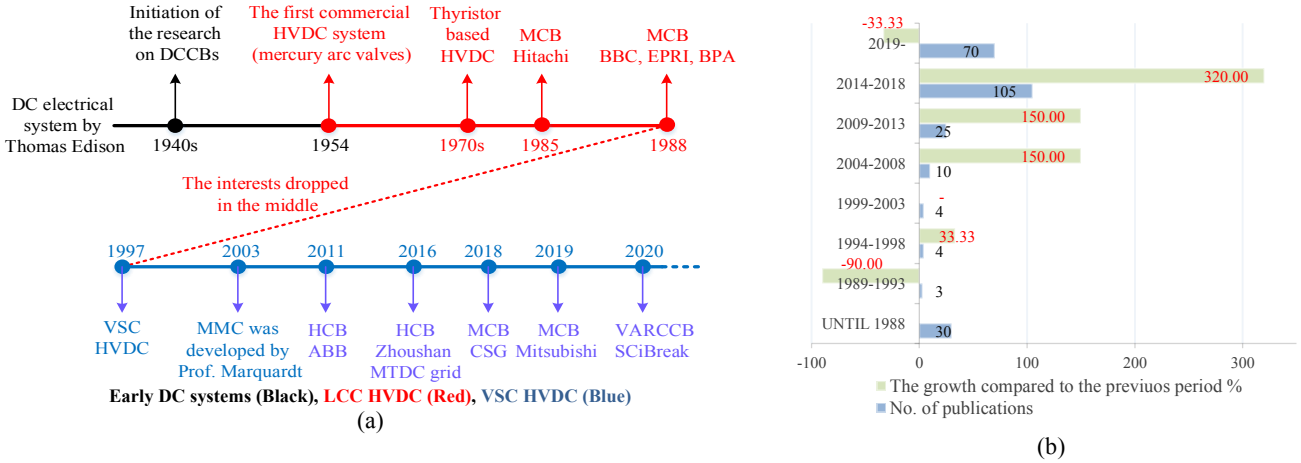

Fig. 1 (a) Timeline for the development of DC CB and (b) General no. of publications on HVDC CBs

Until now, most publications and reports address only a few aspects of the requirements of DC CB in MTDC grids, while this paper provides an overall picture of DC CB technologies in terms of challenges, requirements, time domain simulation, cost and testing considerations. The rest of the paper is organized as follows. Section II summarizes the operation considerations and requirements of DC CB in MTDC grids. Section III deals with the development of DC CB technologies based on the state of art review. The performance analysis of DC CB applications in MTDC grids is presented in Section IV based on time domain simulations and cost related analysis. The remaining challenges and future needs are addressed in Section V, and the paper ends up with meaningful conclusions.

2. Placement, challenges and requirements of DC CB in MTDC grids

2.1. DC CB placement and fault clearing strategies

The DC CB placement and implementation of related protection schemes is tightly related to the converter types, which determine the features of fault current flowing through HVDC system. There are three basic converter topologies: LCC, two-or three-level VSC and MMC [21]. A novel concept, which is based on diode rectifier unit as an offshore converter for offshore wind farm integration [22], belongs to a special case of LCCs. Since the LCC and two-and three-level technologies have some limitations, the MMC technology is commonly accepted as a suitable solution for MTDC grids [23]. Two basic types of MMCs can be easily defined, i.e. (1) non-fault interruption type: the MMC with half bridge submodules, (2) fault interruption type: the MMC with full bridge submodules. According to Cigré technique brochure 739 [24], three types of fault clearing strategies including non-selective, partially selective and fully selective strategies can be considered for an MTDC grid. These strategies are defined in Table 1 together with examples considering the MTDC grid shown in Fig. 2 [25]. AC CBs are installed between the half bridge converter terminals and AC grid, and the DC disconnectors are located in the place to isolate the faulty part in the MTDC grid. This is the traditional protection method that normally leads to the outage of the whole DC systems [26]. In order to avoid power loss in the whole system, the full bridge MMC with a fault interruption function can be adopted, which could suppress the DC side fault current by isolating the fault injection from the AC side [27]. Moreover, by using a DC CB, the faulted sections in MTDC grids could be quickly isolated in a similar way as an AC CB does in the AC grids, which provides better selectivity upon DC fault clearance [28]. With the DC CBs, no special topologies are required for the MMCs, but different control strategies may need to be developed for different MMC types during the faults. Mixed methods could be defined, which for future applications are also likely to provide hierarchical protection with more reliability and much faster restoration capability [29]. It can be seen that DC CBs need to be placed at remote ends of the lines and each side of the nodes for the fully selective fault clearing strategy, which makes the cost very high. In contrast, the cost will be lowest when the non-selective fault clearing strategies are applied with fewer DC CBs. And in the middle, the whole grid can be split into sub-grids (e.g. the two grey circles in Fig. 2) with several DC CBs installed at the borders of these sub-grids when the partially selective fault clearing

strategy is applied [25]. Based on the above discussions, it can be seen that investment costs of DC fault clearance are influenced by the method of DC fault current interruption and the selectivity level of protection strategy.

Table 1 The main fault clearing strategies

Fault clearing strategies in MTDC grids		**Examples (the MTDC grids and related components are in Fig. 2)**
Non-selective	The DC grid is regarded as one protection zone.	The DC fault F1 is cleared by only red elements in the gird, i.e. AC CBs or full bridge converters or DC CBs behind converter terminals.
Partially selective	The DC grid is split into sub-grids, i.e. several protection zones.	Two sub-grids are formed with an insufficient DC CB installation, and F1 is cleared by DC CB4 and DC CB6 installed at the border of sub-grids.
Fully selective	Each DC branch and node are defined as protection zones.	With a sufficient DC CB installations, the fault element is disconnected by the DC CBs at both ends of the element, e.g. F1 is cleared by DC CB4 and DC CB5.

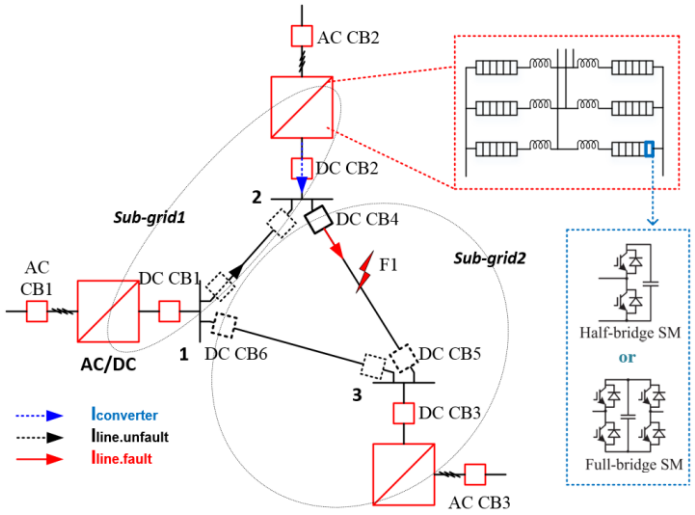

Fig. 2 A simple MTDC grid protected by different fault clearing strategies

2.2. DC CB challenges

2.2.1. DC fault analysis

Prior to addressing DC CB challenges, the related DC fault current analysis in an MTDC grid is of significance. To analyse DC fault current, a pole-to-ground fault is applied on the cable between terminal 2 and terminal 3 in the bipole half bridge MMC based MTDC grid in Fig. 2 with the voltage level of ±320 kV [30]. The fault transient progress can be divided into three stages, which can be observed in Fig. 3 [24] [25] [30] [31]. Iconverter, Iline.fault, Iline.unfault represent the converter output current at terminal 2, the currents flowing through the faulty line and the unfaulty line between terminal 1 and 2.

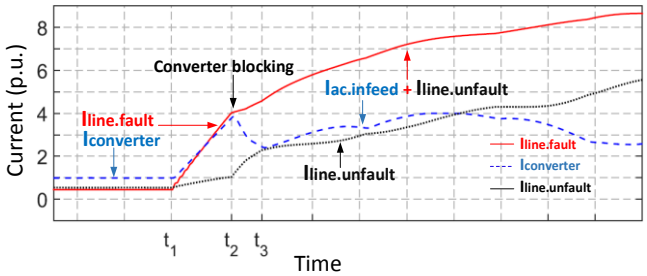

Stage 1. Submodule capacitor discharge period From t_1 to t_2

Stage 2. Arm current decay period From t_2 to t_3

Stage 3. AC infeed period From t_3

Fig. 3 The development progress and stages of DC short circuit currents

After the fault occurs, at instant t_1, travelling waves arrive at the MMC terminal 2 through the faulted line end of the DC reactor, which partly initiate the submodule discharging and then result in a fast current increasing. The converter can still keep its control of the AC side voltages and currents to support the DC fault current rise, until the arm currents violate the threshold of converter blocking at t_2. Since the neighbouring line connected to terminal 2 discharges, the current flowing through the faulty

line ($I_{line.fault}$) rises at a slightly higher rate than $I_{converter}$. After the converter blocks at t_2, the submodule capacitors are bypassed by freewheeling diodes. Hereby, the capacitor discharge is interrupted and the converter cannot keep the control of the AC sides. Since there is no inherent voltage support, only arm reactors keep the current flowing through the diodes. Thus, during Stage 2, the DC current of the converter decays until AC infeed starts at t_3. When the arm currents decay to zero at t_3, the converter is changed to a diode rectifier operation mode; then the DC current results from the AC infeed, i.e. $I_{converter}$ becomes only $I_{ac.infeed}$. Assuming DC CBs and AC CBs have still not interrupted the fault, $I_{line.fault}$ has a higher value than $I_{converter}$, due to the infeed from the neighbouring line ($I_{line.unfault}$). The related general equivalent circuits of Stage 1 and Stage 3 are shown in Table 2 [24] [30] [31]. At Stage 2, only arm currents decaying through arm reactors and diodes are included. The analytical expression of the instantaneous fault current and its rate of rise at Stage 1 are given by (1) and (2), whilst the average DC current in the rectifier operation mode at Stage 3 is expressed by (3).

Table 2 The general equivalent circuits and analytical expressions of fault current in stages [24] [30] [31]

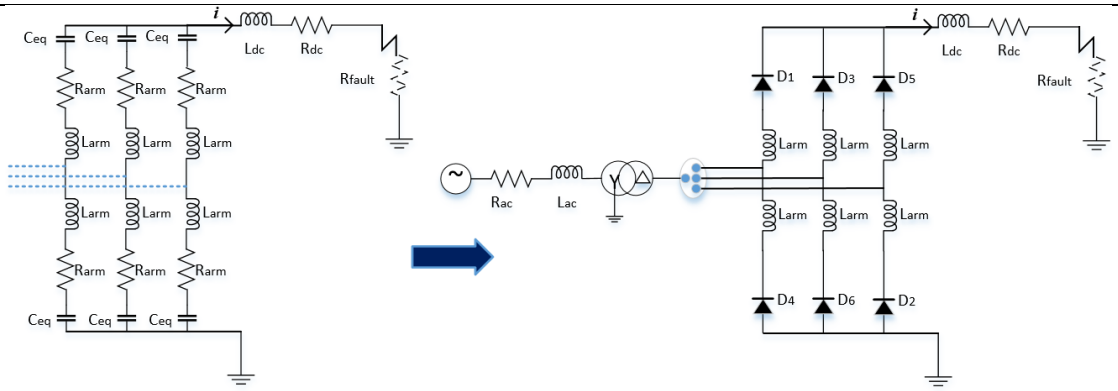

Stage 1. Submodule capacitor discharge period

Stage 3. AC infeed period

$$i(t) = [(Bw - A\alpha)\cos(wt) - (Aw + B\alpha)\sin(wt)]\exp(-\alpha t) \quad (1)$$

$$\frac{di}{dt} = [B(w^2 + \alpha^2)\sin(wt) - A(w^2 - \alpha^2)\cos(wt)]\exp(-\alpha t) \quad (2)$$

where $\alpha = \frac{R}{2L}, w = \sqrt{\frac{dy}{dx} - \left(\frac{R}{2L}\right)^2}, A = CV_{dc}, B = \frac{I_0 + A\alpha}{w}$

$$R = R_{dc} + R_{fault} + \frac{2}{3}R_{arm}, L = L_{dc} + L_{calbe} + \frac{2}{3}L_{arm}, C = 6C_{eq}$$

$$I_{ac,component} = \frac{\frac{2}{\pi}\sqrt{2}V_{ac}}{Z_{total}} \quad (3)$$

where $Z_{total} = Z_{ac} + Z_{tr} + \frac{1}{2}Z_{arm} + \frac{2}{3}(Z_{dc} + R_{fault})$,

Z_{ac}: AC system impedance Z_{tr}: Converter transformer impedance

Z_{dc}: DC side impedance Z_{arm}: Converter arms impedance

From the above analysis of the DC fault current in MTDC grids, it can be seen that the DC parameters will mainly define and influence the transient fault current at Stage 1, and the steady state fault current at Stage 3 is related to both AC and DC side parameters. DC fault characteristics with a high rate of rise of the fault current and without a current zero crossing define the requirements and challenges of the DC CB design, which are very different from those in AC system. Also, creating a current zero in the normal current path for a timely fault current interruption is the primary consideration of the DC CB designs, which is not an issue in the design of AC CBs.

2.2.2. Comparisons and challenges

For both AC CBs and DC CBs, three operation stages can be defined: (1) the breaker opening or the current commutation, (2) the arcing and the energy dissipation and (3) the fault interruption [25]. However, in MTDC grids, DC fault currents are normally characterized by a high rate of rise and the absence of natural current zero crossing points. Due to this high increasing rate, the limitation of the fault clearing time becomes a challenge, which demands a fast breaker to interrupt the fault current

before it rises to uncontrollable levels [32]. The value of the prospective steady state fault current is mainly determined by the AC network strength, and the increase of the DC side inductance will decrease the rate of rise of the DC fault current [33]. These two factors give rise to the requirements and constraints on the selection of the fault clearing strategy and the related DC CB applications. Moreover, the maximum power loss due to a DC fault and the transient stability limits of an AC network should be considered, which provides time related constraints for the DC fault clearance [34]. And the fault clearing times are normally defined in the order of tens of milliseconds, which are regarded as the maximum allowable clearing time concerning power system transient stability [24]. The need for shorter clearing times, however, ranging from 2 to 5 ms are reported in [5].

Another challenge for the DC CB technology originates from the second characteristic of the DC fault currents, i.e., the additional branches are required to help the interruption of the DC fault currents at artificial zero crossing points and the absorb energy stored in the grid. Interrupting the normal load branch current is realized by commutating the current to the additional branches, which imposes a high voltage stress across the DC CB. This high voltage stress results in challenges in design considerations for the normal load branch and the additional branches mainly in terms of insulation strength and short time required for the current commutation. Moreover, during the fault current suppression period, DC CB should withstand a high voltage and a high current at the same time, which is equal to a large amount of energy needed to be absorbed by one of the additional branches [12] [17]. Due to the different mechanism and the development status of the AC CB and the DC CB in a high voltage system, a brief comparison can be seen from the aspects of the breaking current, the interruption time, the reclosing, the production and the standardization in the following table [25] [35]-[38].

Table 3 Comparison between AC CB and DC CB in high voltage systems

	AC CB	**DC CB**
Related break current	• 40/50/63 kA at related voltage 362/500/800 kV	• Up to around 25 kA at 320 kV
The breaking time	• 2 or 3 cycles (50/60 Hz) for voltages below 362 kV • 33 ms for voltages above 500 kV	• About 2 ms to interrupt fault current up to around 25 kA in 320 kV HVDC system
Reclosing requirement and time	• The standard operation sequence is O-t-CO-t'-CO, where O represents Open; CO is Close-Open; t is Reclosing time;	• DC CB at the healthy lines under non-selective protection • For backup operation • As primary protection of overhead lines for self-clearing faults with fully selective protection. • Rapid reclosing might be required in above situations
	• Normal reclosing time 3 min • Rapid reclosing time 0.3 s	• The reclosing time is to be defined in different HVDC system
Production	• Single vendor oriented	• Multiple vendor oriented
Standardization	• Well established methods for testing, e.g. IEEE c37.06, IEC 60255	• No standards for DC grid protection and DC CB

2.3. Operational requirements for DC CBs in MTDC grids

Based on the aforementioned discussions, the operational requirements can be derived as follows:

- Capability to create current zeros and to reliably interrupt the possible maximum fault current in a MTDC grid.
- Shorter clearing time. The total fault clearing time is expected to be shorter than 20 ms, which is associated with the lowest timescales in transient stability limits of connected AC system [34].
- Energy dissipation capability, which should be sufficient to timely dissipate the energy stored during faults.

- Capability to withstand the transient impulse voltage after current interruption.
- Reliable backup protection for breaker failure, which is significant to activate backup breakers with a reasonable current interruption capability.
- Proper coordination among the protection schemes, converter controls and DC CBs, especially in case of a breaker failure.

3. Positioning of DC CB technologies

3.1. General categories of DC CB

Compared to AC CB, the DC CB needs to be modified with additional branches (i.e. commutation branches and energy dissipating branches) to create a current zero crossing or to enforce the DC fault current to zero during current interruption [39], which can be observed in Fig. 4. According to the different types of DC CBs, the mechanism of commutation branch will be different, and the current interruption could occur in a different branch, i.e. the nominal current branch or the commutation branch. Since the DC CB needs to withstand both the high voltage and the high current (i.e. transient interruption voltage (TIV) and peak fault current) during the fault current suppression period, an energy dissipating branch is required to absorb the fault current and to dissipate the energy stored during the interruption process. A typical interruption process of an MCB is shown in Fig. 4 (b) and (c) [7].

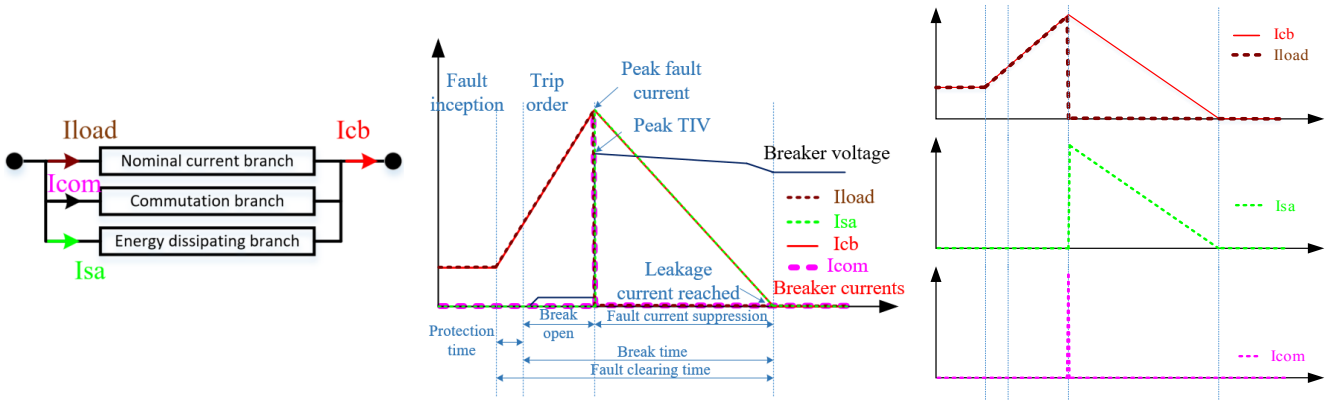

(a) Generic DC CB model (b) DC CB interruption progress (c) Breaker currents

Fig. 4 The generic DC CB model and interruption progress

3.2. Recent Development

There are four main types of DC CBs mentioned in the literatures: MCBs, VARCCB, HCBs and SSCBs [5], which are described as follows:

- MCB-Mechanical circuit breaker

In [39], MCBs are classified as passive resonance and active resonance circuit breakers. The pre-charged capacitor is normally used in the active resonance circuit (in the commutation branch) to create active oscillations instead of self-excited growing oscillations [40]. Different categories can be also made based on the diverse structures and interrupter types. The configuration of a typical active resonance MCB is shown in Fig. 5 (a). In this MCB, the main branch is composed of a mechanical interrupter (VI) and a residual current breaker (RCB). The interrupter can be an oil breaker [41], air-blast breaker

[42], vacuum interrupter [43], or a SF_6 gas breaker [44]. The interrupter is actuated by an ultra-fast mechanical mechanism such as Thomson-coil mechanism to rapidly provide a sufficient contact gap distance, ensuring adequate dielectric strength for the VI so it can endure the transient interruption voltage (TIV). The current injection branch is composed of a resonance circuit including a capacitor (C_p) and an inductor (L_p) in series with an injection switch (S_3). A surge arrester (SA) is connected across C_p and S_3 as an energy dissipating branch. During the current interruption, a short time after receiving the trip order, VI opens and arc current passes through the VI. At the same instant, S_3 closes and pre-charged resonance circuit injects an oscillating current for creating current zeros in the main branch that provides appropriate conditions for the VI interruption. By interrupting the current in VI in one of the artificial current zero points, the breaker current is transferred to the injection circuit for a very short time, which makes the voltage across SA to increase up to its clamping voltage. The current is commutated to the energy dissipating branch. By absorbing the energy in the SA, the current decreases toward zero and RCB opens to interrupt the residual current passing through the MCB.

The whole breaker can be made by one single breaker unit or be the series connection of several individual units with a lower voltage rating [13]. In the classical MCBs, arc features under different conditions, and the parameter optimization of critical capacitors and varistors become important research targets [45] [46]. The requirement for fast interruption is challenging for medium and high voltage breakers, even with an active current injection circuits and vacuum interrupter [32]. Recent development on active current injection MCBs demonstrates 5-10 ms breaking time and interruption capability of up to 16 kA [38] [48].

- VARCCB-VSC assisted resonant current circuit breaker

The configuration of the VARCCB, which can be considered as a novel type of an active resonance mechanical DC CB, is illustrated in Fig. 5 (b). Similar to MCB, the main branch is composed of a vacuum interrupter (VI) which is actuated by an ultra-fast Thomson-coil mechanism, and an RCB. And the dissipating branch is composed of a SA. The current injection branch (i.e. commutation branch) consists of two parts: 1) A resonance circuit composed of a resistor (R_p), a capacitor (C_p) and an inductor (L_p); 2) A VSC composed of four IGBTs, an energy storage capacitor (C_{DC}) and a charging circuit (V_{DC} and R_{CH}). By changing its output voltage polarity in the same direction as the oscillating injection current, the VSC quickly increases the amplitude of the oscillating current. The branch capacitor (C_p) in VARCCB is not pre-charged, which by contrast, is pre-charged in the MCB and the VSC energy storage capacitor (C_{DC}) is pre-charged. The current interruption process of the VARCCB is similar to that of the MCB. The main difference is that the amplitude of the oscillating injection current increases by means of the VSC. Therefore, VARCCB can reach shorter breaking time. Recent development on VARCCB reports 2-8 ms breaking time and an interruption capability of up to 16 kA. Depending on the rated voltage, VARCCB may also be a single unit or consists of the series connection of several individual units [49] [50].

- HCB-Hybrid circuit breaker

The classical configuration of the HCB can be observed in Fig. 5 (c) [40]. When a fault occurs, the trip order arrives at DC CB and then the LCS in the normal load branch turns off. The MB turns on at the same time, then the current is transferred from the normal load branch to the main breaker branch. The UFD starts to open when the current is totally transferred to the main breaker branch. The MB is turned off when the UFD is fully opened and the current is commutated to the energy dissipating branch. The current decreases toward zero by absorbing the energy in the SA, and finally the RCB opens to interrupt the residual current passing through the HCB.

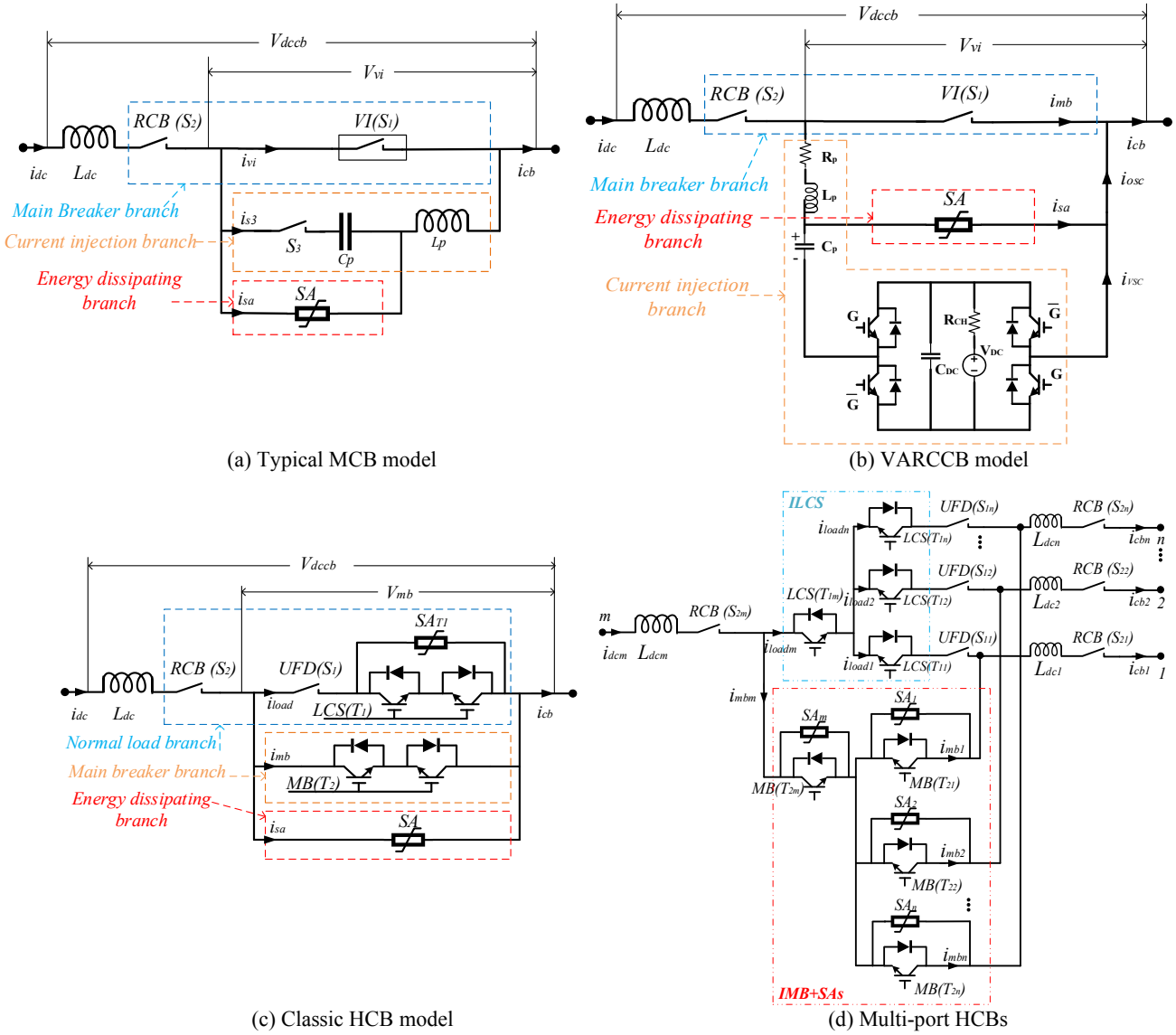

(a) Typical MCB model

(b) VARCCB model

(c) Classic HCB model

(d) Multi-port HCBs

Fig. 5 Typical MCB, VARCCB, HCB and multi-port HCB configurations

It should be noted that here, only system level simplified DC CB models are presented to deal with the general performances, and the component level DC CB models with detailed internal components are not presented, e.g. the cascaded submodules of IGBTs in the branches as described in [40]. As the rating of the most powerful IGBTs is in the order of a few kilovolts and kiloamperes, to withstand TIV and the fault current in MTDC grids, the main breaker branch includes several series and parallel connected IGBT modules. The required number of series IGBT modules depends on the rated voltage while the

required number of parallel IGBT modules is determined by the current interruption capability of the DC CB. As the normal load branch does not expose to high voltages and currents, its required number of series and parallel IGBT modules is lower than that of the main breaker branch. To ensure equal voltage distribution during current interruption, a snubber circuit needs to be installed across each IGBT module. In order to be capable of passing and breaking current in reverse directions, the configuration of series and parallel connected IGBT modules must be capable of passing the current in both directions. Therefore, series and parallel connected stacks of IGBT modules are configured in anti-parallel and anti-series connections. The on-state voltage drop across IGBT modules results in permanent conduction losses in the normal load branch. As there are several IGBT modules in this branch, the conduction losses are low for HCB. Thus, it can be seen that the performance of a typical HCB will be influenced by many factors, e.g. the snubber circuits and stray inductances in the branches, additional bidirectional current interruption capability, cooling system for auxiliary DC breaker and etc. [51]-[54]; and the breaker opening time of HCBs is in the range of 1.2-3 ms [55]. The maximum interruption current reaches 25 kA as reported in [56].

In order to further decrease the capital costs and power losses of HCB, MP HCB have been proposed [57] [58]. A typical MP HCB can be seen in Fig. 5 (d) with an integrated main breaker (IMB), an integrated load communication switch (ILCS), more UFDs and RCBs. The general idea is to share the common branches within multiple ports connected to the same DC bus. Port m is connected to a DC bus, and ports 1 to n are connected to adjacent transmission lines. However, this MP HCB is highly complex and difficult to guarantee the correct operations when the common parts are broken, e.g. the RCB, LCS and MB at the m side.

Besides classic HCBs and related MP HCBs, several new HCB and MP HCB topologies are proposed recently in the literature [59]-[64], only some of which are realized by low voltage prototypes. As an example, a new HCB characterized by mixed connection of thyristors and IGBT half bridge submodules in the main breaker is proposed in [59]. Since thyristors can endure a major part of TIV, the number of required full-controlled power semiconductors is reduced leading to the cost reduction of the HCB. The breaking time of the proposed HCB is a bit longer than that of a full-controlled semiconductor-based HCB. Another HCB called T-type HCB which is based on cascaded half bridge submodules is introduced in [60]. The T-type HCB uses a main breaker branch composed of cascaded half bridge submodules and diode strings instead of a conventional main breaker parallel to an LCS in a classic HCB. This topology reduces the number of required IGBTs and it can decrease the fault peak current and the breaking time.

Some other topologies are proposed to integrate dc current flow control function inside MP HCB [65] [66]. The current flow control is required in MTDC grids in order to prevent the lines from being overloaded. Several power electronic based current flow controllers, such as variable resistors [67], dc/ac converters [68] and dc/dc converters [69], are proposed for this purpose. Integrating a current flow controller inside the dc breakers reduces the costs of these solutions. An MP HCB equipped with full bridge submodules simultaneously operating as both LCS and current flow controller and capable of blocking the

current is proposed in [65], where the submodules of the LCSs installed at adjacent lines are connected in parallel. A similar topology is presented in [66].

It should be noted that the SSCBs can be regarded as pure semiconductor switches without using any mechanical switch, which have very short breaking time but with high costs and conduction losses [49] [70]. Therefore, it is not considered as a practical solution especially in high voltage levels and is not considered in this paper.

4. Performance analysis for DC CB applications in future MTDC grids

4.1. Time domain simulation based performance comparison between different types of DC CB

In this section, four types of DC CBs are adopted for the comparison of fault current interruption, which are:

- MCB model, as shown in Fig. 5 (a),
- VARCCB, as shown in Fig. 5 (b),
- HCB, as shown in Fig. 5 (c),
- MP HCB, as shown in Fig. 5 (d).

The related parameters of these four types of DC CBs and test systems can be found in [40] [71] [72] respectively. The related DC voltage and interrupting current are 320 kV and 16 kA. The MP HCB is developed based on HCB, in which the parameters and the topologies of the selected HCB will be adopted and improved. The circuit for verifying the validity of the single-port DC CB models, i.e. MCB, VARCCB and HCB, is shown in Fig. 6 (a). An ideal DC source, a resistive load and two cable branches are used in this circuit to test the target DC CB models. A revised verification circuit with one more cable branch to validate MP DC CB model is given in Fig. 6 (b).

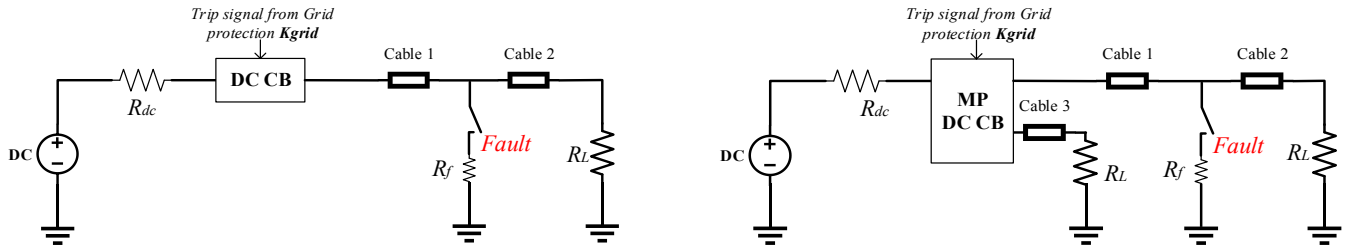

(a) A simple verification circuit for single-port DC CBs (b) The revised verification circuit for MP DC CBs

Fig. 6 The verification circuits for testing typical DC CB models

The time domain simulations based on PSCAD/EMTDC is adopted here for the validation of system level DC CB models [73]. The simulation results of the interruption progress can be observed in Fig. 7. The signals with subscripts M, V, and H represent the related variables in MCB, VARCCB and HCB, respectively. The fault occurs at 0.1s and it is located between cable 1 and cable 2. Then, the trip order Kgrid from grid protection will be received by DC CB at 0.102s, as shown in the first row of Fig. 7. The current waveforms of MCB, VARCCB and HCB during the fault interruption can be observed from the middle rows of Fig. 7 respectively. The result comparisons between three types of DC CBs can be easily observed by the corresponding waveforms in the same scales. The current zeros of the load branch currents (Ivi_M, Imb_V and $Iload_H$) during the cases with MCB, VARCCB and HCB occur around 0.1101s, 0.1048s and 0.103s, before the SAs start to dissipate the energy.

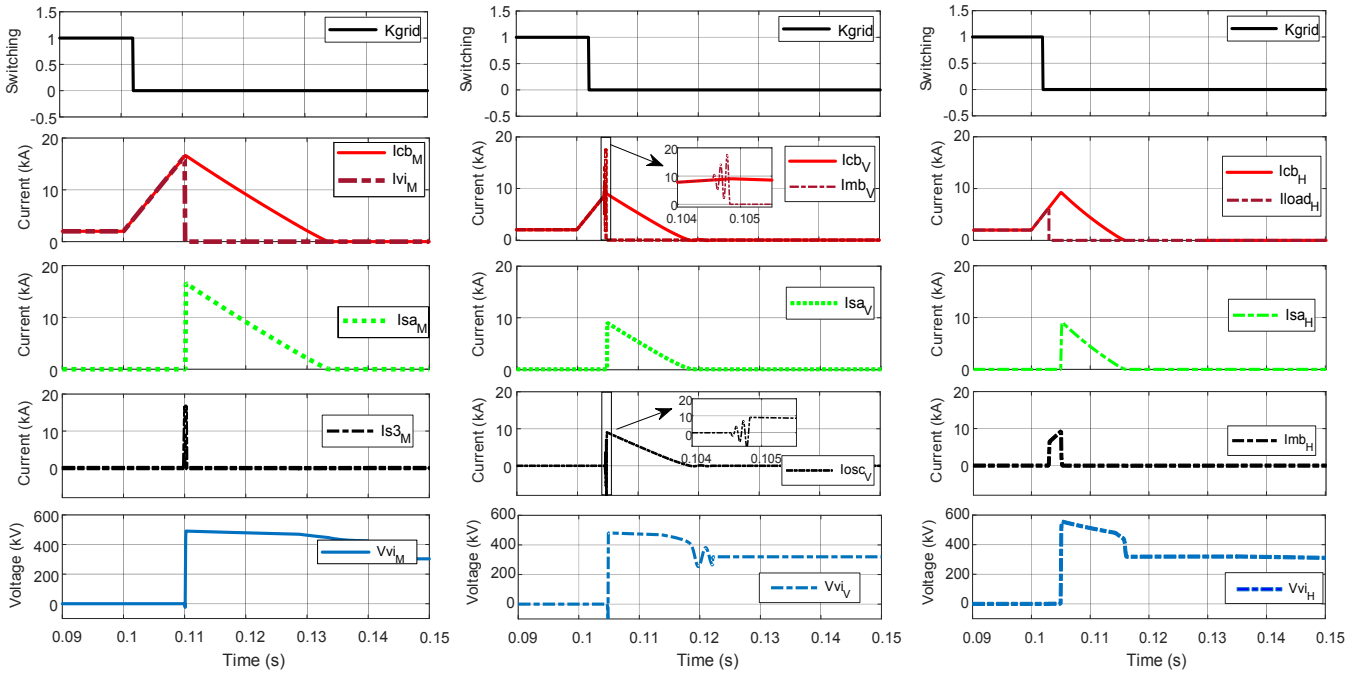

(a) Interruption waveforms of MCB (b) Interruption waveforms of VARCCB (c) Interruption waveforms of HCB

Fig. 7 Simulation results of typical DC CB models in the test circuits

From the fourth row of Fig. 7, the differences of the commutation currents express the different current interruption mechanisms of MCB, VARCCB and HCB. The comparisons of dissipating branch currents and load branch voltages can be observed in the third and fifth rows of Fig. 7. It can be observed that the oscillating injected current in VARCCB ($Iosc_V$) gets the zero crossing point earlier than the injection current in MCB ($Is3_M$), and at the almost the same moment as the current (Imb_H) in HCB are transferred from commutation branch into the related energy dissipating branch. But with different characteristics of SAs, the current in HCB (Isa_H) decrease faster than the current in the VARCCB (Isa_V). Since the MP HCB is developed based on HCB and related parameters, almost the same performances can be obtained. The voltages of VIs (and load branches) and the energy dissipated by those SAs are different, because of the different interruption time, SA parameters and oscillation circuits. The related differences can also been observed in Table 4 with more information from [14] [21] [32] [55] [74].

Table 4 Comparison of different types of DC CB

	Classic HCB	**MP HCB**	**VARCCB**	**MCB**
Nominal current branch	UFD and IGBT based LCS	UFD and IGBT based LCS	VI	VI
Commutation branch	IGBT based main breaker	IGBT based main breaker	VSC and LC based injection circuit	LC based injection circuit
Interruption mechanism	The current flowing through nominal current branches is transferred into the main breaker branch to interrupt	The current flowing through nominal current branches is transferred into the main breaker branches to interrupt	The VSC injects the oscillation current with increasing amplitude in every half cycle to create a zero in nominal current branch for VI interruption	The pre-charged injection circuit injects the current for creating a current zero in nominal current branch for VI interruption
Max. interruption current (kA)	16-25	16-25	9-16	16
Breaking time (ms)	2-5	2-5	2-8	5-10
On state losses	High	High	Low	Low
Development state	320 kV Prototype, 500 kV under development	Under research for 320 kV	27 kV and 80 kV prototypes, under research for 320 kV	160 kV in operation
TIV (p.u.)	1.6	1.6	1.51	1.53
Dissipated energy (MJ)	Low	Low	Low	High

4.2. Placement of DC CB in MTDC grid with considerations of DC CB cost and FCS selectivity

An economic comparison of SSCB, MCB and two types of HCBs has been given in [75], with the consideration of voltage ratings. Based on the comparative analysis in [76], the practical implementation of DC CBs will mainly consider the following factors: voltage rating, interruption time, power losses, maximum interruption current and cost. The Cigré technique brochure 533 reported a system level cost analysis of HVDC system and related DC CB implementation, where the costs of station losses and DC CB with different converter station topologies have been considered [21]. The cost of one 320 kV breaker is at least not more than one sixth of a +/-320 kV converter's cost, and a 1500 MW converter station costs about 150 MEUR [21]. Also the different choices of main components in the critical branches are considered to present the cost differences of the DC CBs at the system level, which can be observed in Table 5 [74]-[82].

Table 5 Approximate cost comparison of different types of DC CB

		Classic HCB [76]-[78]	**MP HCB [81]**	**VARCCB [49] [50] [80]**	**MCB [75] [80]**
Voltage rating (kV)		320	320	320	320
Topology consideration	*Nominal current branch*	3x3 IGBTs in LCS	In Fig. 5 (b), 3x3x4 IGBT in ILCS	VI	VI
	Commutation branch	160 IGBTs in MB	160x4 IGBTs in IMB	IGBT (3x4x4) based VSC injection circuit	LC based injection circuit
	Energy dissipating branch	Metal Oxide SA	Metal Oxide SA x4	Metal Oxide SA	Metal Oxide SA
Cost		Very high	High	Medium	Low

For the suitable implementation at the required voltage ratings (e.g. 320 kV), one DC CB can comprise several series connected basic DC CB modules with lower ratings (e.g. 80 kV) [78]. For example, the HCB with ratings 80 kV and 2 kA can be set with 3x3 IGBTs in LCS and 40 IGBTs in MB, considering the selected BIGBT module (4.5 kV and 3 kA) [79]. And for a 320 kV/2 kA HVDC, the HCB could be comprised of four cascaded 80 kV HCB modules (i.e. 3x3x4 + 40x4 IGBTs), or composed in the branch level (i.e. one LCS and four 80 kV MBs with 3x3 + 40x4 IGBTs). The number of IGBTs will be doubled when the bidirectional operation is considered. The MP HCB considers that a more cost-efficient combination in the branch level, e.g. the one in Fig. 5 (b) and Table 5, is designed and more suitable for a four-port system with LCS, MB and SA branches integrated and shared between every two ports.

Even though there are different DC CB solutions, when HV electrical systems and related protection systems are considered with the selectivity of FCS, the placement of DC CB system can be further investigated [24], which can be conducted by the working flow in Fig. 8.

A symmetric monopole three terminal HVDC grid with half bridge MMC, as depicted in Fig. 2, is chosen to study here, in which the half bridge MMC is without fault interruption functions and one DC CB is assumed to install at the converter terminal. Then, the required number of DC CBs for different FCS is provided in Table 6. Here, for each option of FCS, only the application cases with typical DC CBs are chosen for a general comparison, thus the AC CB based non-selective FCS will not be considered here. For partially selective FCS, the triangle HVDC transmission topology can be at least divided into two sub-grids with two more DC CBs (the case in Fig. 8), and at most five zones with five more DC CBs (when one line and one bus are

covered by one zone). It can be seen from Table 6 that the selectivity of FCS will be largely determined by the DC CB's number and placement, and the cheapest FCS is the non-selective one with least placement of DC CBs and lowest selectivity.

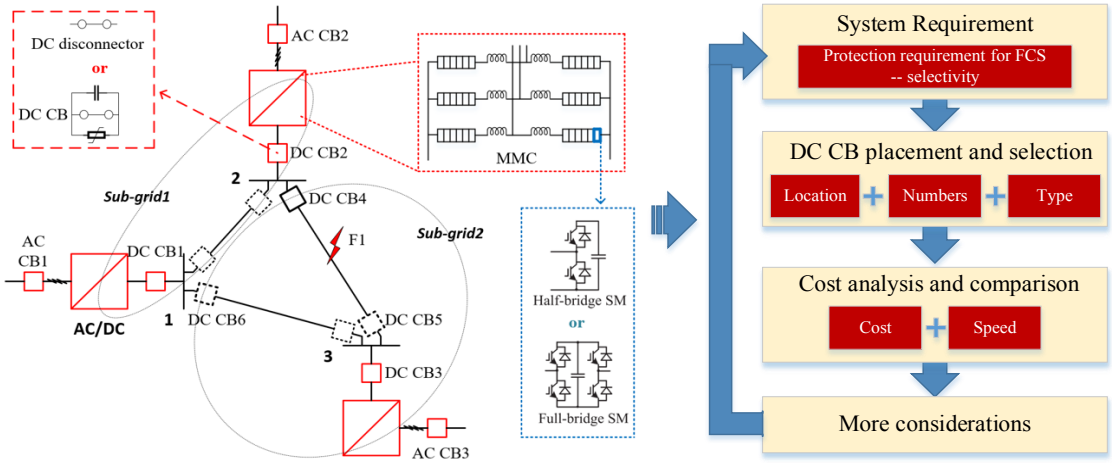

Fig. 8 The working flow of a cost based DC CB planning considering FCS in MTDC grid

Table 6 The required number of DC CBs for different fault clearing strategies

	Options of FCS		*DC CB placement*	*No. of DC CBs (n)*
1	Full selective FCS	6 protection zones	At each end of DC branches and buses	18
2	Partially selective FCS	5 protection zones	At borders of protection zones, and the number of zone will decrease when one zone cover more branches and buses, e.g. 2 zones are composed in Fig. 8, only DC CB4, DC CB6 and DC CB3 installed in sub-grid2, and only DC CB1 and DC CB2 in sub-grid1.	16
		4 zones		14
		3 zones		12
		2 zones		10
3	Non-selective FCS	1 zone in the grid	Only DC CBs at converter sides are installed, e.g. DC CB1, DC CB2 and DC CB3.	6

Apart from the selectivity, which depends on the number of protection zones and DC CBs, the cost and speed cannot be easily defined. When a full selective FCS is required with the implementation of 18 DC CBs, the solution with MCB are much cheaper than the one with HCB, and the lower speed of MCB could be accepted. However, with newly developed VARCCB, a lower cost increment than HCB can obtain higher speed than the MCB solution. Moreover, if the full selective FCS is considered with MP HCB implementation, the cost will be largely decreased from the classic HCB solution, and the speed performance will be better than MCB and VARCCB solutions. Thus, from both perspectives of cost and speed, the VARCCB and MP HCB solution will be better than other solutions.

Considering that there is still a large cost difference between VARCCB and MP HCB solutions, more cost considerations on the requirement of on-state losses, system stability constraints, DC CB related parameter optimization and control system complexity need to be further investigated [21] [75]. Also the cost and the speed related performance and criteria of DC CBs would change because of market situation and technology innovation, and different DC CBs will be exposed to different risks, e.g. the possible failure of common switches in MP HCB and diverse difficulties during repeated fault interruption and reclosing [49] [82]. When the system wide coordinative protection and control are considered, the different issues between converter control, fault current limiter and AC CB/DC CB based protective control during fault clearing and system recovering will be complicated and significant [24]. Thus, for future investigation, besides the selectivity, cost and speed, more factors related to

the reliability and robustness of those new solutions (such as [65] [66]) in a system wide level could be of importance [52], which can help find the most suitable solution for the security of future MTDC grids.

5. Coordination and testing investigation of DC CB in future MTDC grids

5.1. Reclosing and recovering function

In order to ensure power system security and stability, the MTDC grids must be able to quickly recover power transmission after fault clearing. Subsequent to isolation of overhead lines in case of a transient fault, the DC CBs need to do reclosing in order to recover power transmission. In the conventional reclosing strategy, the DC CBs will automatically re-close within a predefined time in order to ensure the arc deionization of a faulted overhead line. The time sequence of conventional reclosing is shown in Fig. 9. However, re-closing under permanent fault will deteriorate overcurrent issues in the MTDC grids, which raises a high requirement of the DC CB interruption capacity [83]. To prevent re-closing under permanent fault, adaptive reclosing schemes have been proposed to determine the suitable reclosing operations for different fault types, i.e. permanent or transient. An adaptive reclosing scheme with HCBs, using active voltage pulse injection from the associated converter, is proposed in [84]. A similar method based on active pulse injection using hybrid MMC, including both half bridge and full bridge submodules in the arms, is proposed in [85]. Two fault type identification methods based on measuring line residual voltage are proposed in [86] [87]. In these methods, only RCB is required to be reclosed for fault type identification, and therefore they can be applied in case of MCB and VARCCB.

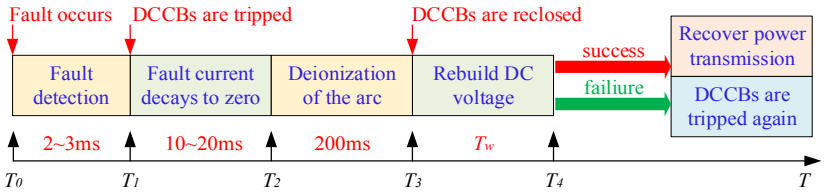

Fig. 9 The time sequence of conventional reclosing [84]

In order to avoid potential adverse impacts such as mal-operation of the protection system, line insulation failure, and to reduce stresses on power electronic devices resulting from reclosing DC CBs in one stage, sequential or soft reclosing schemes have been proposed in [88][89]. These schemes make use of controllable cascaded submodules in the commutation branch of HCB. And the rate of rise of voltage and current are limited by step-by-step operation of the submodules in commutation branch of HCB. The DC voltage at the line side of HCB is checked to determine if the fault is eliminated or it is permanent. The schemes can be implemented at both ends of the line and eliminate the need for communication links between line ends used for reclosing. Moreover, multiple auto-reclosing operations can be conducted since the dissipated energy is negligible here.

5.2. Testing requirements and considerations

Currently, there are no standards on test requirements and procedures of DC CBs. Simultaneous presence of voltage and current of the DC CB during current interruption results in energy absorption requirement and therefore the testing of DC CB is

fundamentally different than that of AC CB. Meaningful validation of DC CBs can be made when the tests accurately reflect practical conditions occurring in real HVDC systems. Generic test requirements can be categorized into four types, i.e., dielectric, operational, breaking and endurance tests [30] [31]. The short circuit current breaking test is the most important and challenging one, since there is a high requirement of a sufficient capability for supplying high rising rates of fault current.

For the basic concept and topology validation, offline electromagnetic transient simulation is normally used, which may have impractical simulation time and simplified models [90]. Multi-physics simulation can also be adopted when the plasma and thermal effects have been considered in DC CB modelling [91] [47]. Since HVDC CBs are very expensive and interact strongly with the related DC protection and MTDC grids, power-hardware-in-the-loop (PHIL) methods become popular to test the system level cooperation performances of DC CBs and protection, where complex HVDC system operation conditions can be simulated and the DC CB prototypes are normally built in a low power level [12] [92]. In PHIL testing methods, a suitable power amplifier will be applied to generate the required short circuit voltage and current for testing DC CB prototypes, which is not needed during the offline simulation and validation stages.

The full power testing of DC CB prototypes could be conducted in the synthetic testing [93]. Due to the lack of HVDC synthetic test circuit design experiences, the standard of AC synthetic test is normally adopted as the reference of DC synthetic test method design. Several synthetic DC CB test circuits are investigated in [40] [94] [95]. A synthetic test circuit composed of AC short circuit generators operating at low frequency is proposed by KEMA [96], as shown in Fig. 10. The test circuit provides all the generic requirements and it can be used for full power testing of DC CBs, especially when the breaking process is much shorter than the half cycle of generators' voltage. Moreover, the ac short circuit generators are already available because they are being used for ac equipment testing. As shown in Fig. 10, the test circuit comprises four parts, including power source part, overcurrent protection part, a dc voltage source part for dielectric stress and an arcing time prolongation circuit part. The power source part, which is formed of low frequency ac short circuit generators and power transformers, supplies the required current, voltage and energy during the current interruption. The overcurrent protection part, including a plasma triggered spark gap (TSG1) and an auxiliary HVAC SF_6 breaker (AB1), protects the test object (TO) and/or the components of the test circuit in case of DC CB operation failure. The DC voltage source part, which is made up of an AC source, a diode, a capacitor, an inductor, a plasma triggered spark gap (TSG3), and a HV AC CB (AB2), applies TIV after current breaking. The arcing time prolongation part provides an additional arcing time for AB1 to build the required test current with a specific rate of rise.

According to above discussions and considerations, the related comparisons between different simulation and testing methods on validation stages, focuses, requirements and capabilities can be observed in Table 7.

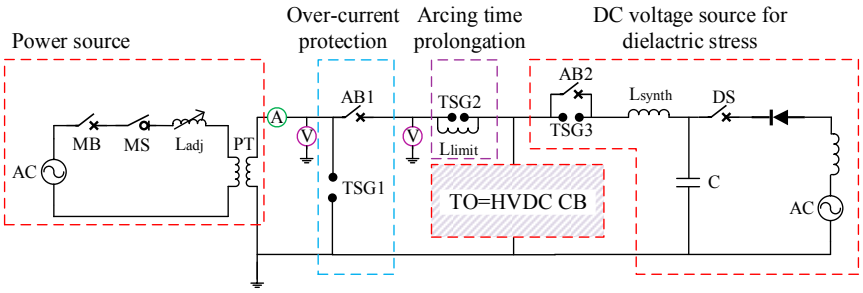

MB = Master Breaker
MB = Making Switch
L_{adj} = adujustable reactor
PT = Power Transformer(s)
AB = Auxiliary AC breaker

L_{synth} = Inductance in the synthetic circuit
DS = Disconnector Switch
TSG = Triggered Spark Gap (Triggered make gap)
L_{limit} = initial current limiting reactor

Ⓐ = Current measurement
Ⓥ = Voltage measurement
TO = Test object
C = Capacitor bank

Fig. 10 The circuit for testing DC CB performance [96]

Table 7 Comparisons between different simulation and testing methods

	Offline simulation	**Multi-physics simulation**	**PHIL testing**	**Full power testing**
Validation stage	Basic concept and topology level	Detailed component level	Prototyping and partly prototyping level	Final product level
Validation focus	• Electromagnetic transient simulation	• Electromagnetic transient • Arc plasma • Thermal progress	• Complex simulation scenarios • Cooperative operation test • Related operation limits	• A synthetic test including all focuses • Security, reliability, and compatibility, etc.
Requirements	• Simulated testing conditions • Concept level/ component level DC CB models	• Simulated testing conditions • Specific component level DC CB models	• Simulated testing conditions • Specific component level DC CB models • Low power prototype or part of the prototype • Effective power amplifier to generate the short circuit current	• A synthetic test circuit composed of ac short circuit generators to provide short circuit current • Related protection for test circuit • DC voltage source for testing dielectric stress • Arcing time prolongation circuit • Full-pole DC CB prototype
Capability	Current breaking test	Dielectric, breaking and endurance tests	Dielectric, operational, breaking and endurance tests	Dielectric, operational, breaking and endurance tests

6. Remaining challenges and future needs

According to the presented details concerning DC CB applications in HVDC power systems, several main technological areas have been investigated and discussed, where further research and development is still required to improve the DC CB capabilities to deal with the remaining challenges. Four main areas are summarized as follows:

6.1. The breaker architecture and multi-physic simulation

In order to make a reliable configuration of a DC CB, its architecture must be accounted, as the DC CB normally consists of electrical, mechanical, and thermal components. The operation of such a complex system results in different physical phenomena. Therefore, comprehensive analysis and design of a DC CB requires multi-physical and/or finite element based models that can predict the different phenomena and characteristics with a required degree of accuracy, in order to investigate the effects related to the mechanical structure, acoustics, electromagnetic coupling and heat transfer. As a result, the architecture of a DC CB can be optimized.

6.2. Coordination with protection, control and fault clearing strategies

It can be seen from the previous discussions that DC fault characteristics are defined by AC and DC system parameters and related fault current control strategies [97], which are challenging for the design and testing of DC CBs. Especially for the reliability of the whole MTDC grid, the reclosing and recovering functions are also required as parts of DC system protection strategies. All these considerations and requirements express the significance of the coordination between the DC CB and the protection and control strategies during the planning, design and operation stages of DC CBs and protection systems. In addition, since the interactions between converter fault controls and DC reactor designs depend on different converter topologies and ratings, the system level coordination between DC CB based protection system, MMC based control system and MTDC grid configurations are important to realize the effective fault clearing and post fault recovering. The global optimization of the whole system, including DC CB, control and protection, is expected in the future designs and operations of MTDC grids.

6.3. Synthetic evaluation system for DC CB modelling and reliable operation

Due to the increasing complexity of DC CB modelling and related system level interactions, the performance evaluation need to be redefined according to the dimensions of the DC CB multi-physics models. Moreover, different kinds of failure modes in different levels can be developed for both internal and external interactions of DC CBs, e.g. the interruption failure of VI in MCB or coordination failure between DC CB and converter fault control. Thus, such a challenge necessitates to identify the possible failure models of existing DC CB technologies in the related synthetic evaluation system for a reliable fault clearing in future HVDC grids.

6.4. Testing and standardization

In addition to the synthetic testing of full-pole DC CBs, the multi-layer test system can be used in a way to test the HV DC CB component by component, branch by branch, unit by unit, and then it can be upgraded for a HVDC system level application testing. The reliability testing on common branches, especially in case of MP HCB, will define final quality and feasibility of DC CBs. In this way, the mechanism and the concepts for both component level and system level can be thoroughly validated by applying appropriate evaluation systems, which can provide sufficient information in order to perform DC CB design optimization, standardization and industrial production. Considering that different DC CBs and HVDC solutions from more than one manufacturer may exist in the new MTDC grids, the interoperability issues cannot be ignored as well. Standardizations for the MTDC grids and related protection systems are particularly significant, especially for DC CBs and their coordination with the power network and protection systems.

7. Conclusion

In this paper, an overview on the development and challenges of HVDC circuit breaker technologies is presented, which pave the way for future applications. As an important component to secure the operation of MTDC grids, DC CBs have been under the research and the development since 1940s for different generations of HVDC systems. Compared to AC CBs, the operations and requirements of DC CBs are different due to the complexity of modern hybrid AC-DC power systems and related

control strategies. The classical types of DC CBs have been investigated and compared, based on literature overview, time domain simulation and cost analysis. By taking into account protection strategies with different selectivity requirements, the optimal solutions of DC CBs can be defined according to the cost optimization functions. The reclosing and recovering functions of DC CBs have also been discussed in this paper, and they deserve more attentions with respect to protection and control operation of the future MTDC grids. Moreover, more intelligent and comprehensive evaluation and testing systems are required for the DC CBs as they will be the basis for future standardization related to MTDC grid operation.

References

[1] Li, H., Chen, Z.: 'Overview of different wind generator systems and their comparisons', *IET Renewable Power Generation*, 2008, **2**, (2), pp. 123–138.

[2] ABB, "Québec - New England, The first large scale multiterminal HVDC transmission in the world to be upgraded", 2016. [Online]. Available: https://new.abb.com/ systems/hvdc/references/quebec-new-england

[3] Bathurst G. and Bordignan P.: 'Delivery of the Nan'ao multi-terminal VSC-HVDC system,' *Proc. 11th IET International Conference on AC and DC Power Transmission*, 2015, pp. 1-6.

[4] Tang, G., He, Z., Pang, H., Huang, X., Zhang, X., 'Basic Topology and Key devices of the Five-Terminal DC grid', *CSEE Journal of Power and Energy Systems*, 2015, **1**, (2), pp. 22-35.

[5] Li, G., Liang, J., Balasubramaniam S., and Joseph T., et al: 'Frontiers of DC Circuit Breakers in HVDC and MVDC Systems', *Proc. 2017 IEEE Conference on Energy Internet and Energy System Integration,* 2017, pp. 1-6.

[6] Greenwood, A., Kanngiessner, K., Lesclae, V., Margaard, T., and Schultz, W., 'Circuit breakers for meshed multiterminal HVDC systems Part I: Introduction DC side substation switching under normal and fault conditions', *Electra*, 1995, **163**, pp. 98–122 .

[7] Liu, S. and Popov, M.: 'Development of HVDC system-level mechanical circuit breaker model', *International Journal of Electrical Power & Energy Systems,* 2018, **103**, pp. 159-167.

[8] Pei, X., Cwikowski, O., Vilchis-Rodriguez, D. S., and Barnes, M., et al.: 'A review of technologies for MVDC circuit breakers', *Proc. IECON 2016 - 42nd Annual Conference of the IEEE Industrial Electronics Society*, Florence, 2016, pp. 3799-3805.

[9] Z. Zhang, X. Li, M. Cheng, et al. 'Research and Development of an Ultra-fast 160kV Mechanical HVDC Circuit Breaker', *Power System Technology*, 2018, **42**, (7), pp. 2331-2338.

[10] Wikipedia, 'Thomas Edison', 2019. [Online]. Available: https://en.wikipedia.org/wiki/Thomas_Edison

[11] Brückner, P.: "Abschalten einer in Betrieb befindlichen Gleichstromleistung". Germany Patent B 207 592, 20 November 1944.

[12] Franck, C. M.: 'HVDC Circuit Breakers: A Review Identifying Future Research Needs', *IEEE Transactions on Power Delivery,* 2011, **26**, (2), pp. 998-1007.

[13] Tokuyama, S., Arimatsu, K., Yoshioka, Y. and Kato, Y. 'Development and interrupting tests on 250 KV 8 KA HVDC circuit breaker', *IEEE Transactions on Power Apparatus and Systems*, 1985, **104**, (9), pp. 2452–2459.

[14] Pauli, B., Mauthe, G., Ruoss, E. and Ecklin, G. 'Development of a high current HVDC circuit breaker with fast fault clearing capability, ' *IEEE Transactions on Power Delivery*, 1988, **3**, (4), pp. 2072-2080.

[15] Asplund, G., Svensson, K., Jiang, H., Lindberg, J., Pålsson, R., 'DC transmission based on voltage source converters', *CIGRÉ session*, Paris, 1998, paper ref. 14-302.

[16] Lesnicar, A. and Marquardt, R.: 'An innovative modular multilevel converter topology suitable for a wide power range', *Proc. IEEE Power Tech Conference*, Bologna, 2003.

[17] Häfner, J. and Jacobson, B.: 'Proactive hybrid HVDC breakers – A key innovation for reliable HVDC grids', *Proc. CIGRÉ Bologna Symposium*, Bologna, 2011.

[18] Jie, Z., Haibin, L., Rui, X., Li, L., Wenhai, N., et al.: 'Research of DC circuit breaker applied on Zhoushan multi-terminal VSC-HVDC project'. *IEEE PES Asia-Pacific Power and Energy Engineering Conference (APPEEC)*, 2016, pp. 1636-1640.

[19] *Mitsubishi Electric Achieves Successful Fault Current Interruption using 160kV DC Circuit Breaker*. Available: https://www.mitsubishielectric.com/news/2019/1010-a.html

[20] *SCiBreak 80 kV modular HVDC breaker successfully tested at KEMA*. Available: https://www.scibreak.com/?p=95121

[21] CIGRÉ Working Group B4.52, 'HVDC Grid Feasibility Study', TB-533, 2013, www.e-cigre.org.

[22] R. Li, L. Yu, L. Xu, G. P. Adam, 'DC Fault Protection of Diode Rectifier Unit Based HVDC System Connecting Offshore Wind Farms", *IEEE Power & Energy Society General Meeting (PESGM),* 2018, pp. 1-5.

[23] Oni, O. E., Davidson, I. E. and Mbangula, K. N. I.: 'A Review of LCC-HVDC and VSC-HVDC Technologies and Applications', *IEEE 16th International Conference on Environment and Electrical Engineering*, Florence, 2016.

[24] CIGRÉ Working Group B4/B5-59, 'Protection and local control of DC grids', CIGRÉ TB-739, 2018.

[25] Liu Z., Mirhosseini S. S., Popov M., Audichya Y., Colangelo D., Jamali S., et al., 'Protection Testing for Multiterminal High-Voltage dc Grid: Procedures and Procedures and Assessment,' *IEEE Industrial Electronics Magazine*, 2020, **14**, (3), pp. 46-64.
[26] Dantas, R., Liang, J., Ugalde-Loo, C. E., and Adamczyk, A., et al.: 'Progressive Fault Isolation and Grid Restoration Strategy for MTDC Networks', *IEEE Transactions on Power Delivery,* 2018, **33**, (2), pp. 909-918.
[27] Wenig, S., Goertz, M., Hirsching, C., and Suriyah, M., et al.: 'On Full-Bridge Bipolar MMC-HVDC Control and Protection for Transient Fault and Interaction Studies', *IEEE Transactions on Power Delivery,* 2018, **33**, (6), pp. 2864-2873.
[28] Johannesson, N., Norrga, S. and Wikstro M, C.: 'Selective Wave-Front Based Protection Algorithm for MTDC Systems', *Proc. 13th International Conference on Development in Power System Protection 2016 (DPSP)*, Stevenage, 2016..
[29] Zhang, L., Zou, Y., Yu, J., and Qin, J., et al.: 'Modeling, control, and protection of modular multilevel converter-based multi-terminal HVDC systems: A review', *CSEE Journal of Power and Energy Systems,* 2017, **3**, (4), pp. 340-352.
[30] Belda N. A., Plet C. A., and Smeets R. P. P., 'Analysis of faults in multiterminal HVDC grid for definition of test requirements of HVDC circuit breakers', *IEEE Transactions on Power Delivery*, 2018, **33**, (1), pp. 403–411.
[31] Belda N. A., Plet C. A., Smeets R. P. P., and Nijman R., 'Stress analysis of HVDC circuit breakers for defining test requirements and its implementation', *Proc. CIGRE Colloquium*, 2017, pp. 1-11.
[32] CIGRÉ Joint Working Group A3-B4.34, 'Technical Requirements and Specifications of State-of-the-art DC Switching Equipment', CIGRÉ TB-683, 2017, www.e-cigre.org.
[33] Li, B., Jing, F., Li, B., and Wen, W.: 'Research on the Parameter Matching Between Active SI-SFCL and DC Circuit Breaker in DC systems', *IEEE Transactions on Applied Superconductivity,* 2019, **29**, (2), pp. 1-5.
[34] CENELEC TC 8X/WG 06, 'System Aspects of HVDC Grids', *CENELEC*, 2016, https://www.cenelec.eu
[35] IEEE P. &. E. Society, 'IEEE Std C37.06 for AC High-Voltage Circuit Breakers Rated on a Symmetrical Current Basis-Preferred Ratings and Related Required Capabilities for Voltages Above 1000 V', Std., 2009.
[36] Storasta, L., Rahimo, M., Haefner, J., and Dugal, F., et al.: 'Optimized power semiconductors for the power electronics based HVDC breaker application', *Proc. PCIM Europe 2015*, 2015, pp. 1–6.
[37] Skarby, P. and Steiger, U., 'An ultra-fast disconnecting switch for a hybrid HVDC breaker - A technical breakthrough', in *Proc. CIGRÉ Session*, Alberta, Canada, Sep. 2013, pp. 1–9.
[38] K. Tahata, S. El Oukaili, K. Kamei, D. Yoshida, Y. Kono, R. Yamamoto, and H. Ito, 'HVDC circuit breakers for HVDC grid applications', *in Proc. AORC-CIGRÉ*, Tokyo, Japan, 2015.
[39] Margi, U., Priyank, S.: 'A Review on HVDC Circuit Breakers', *International Journal of Engineering And Computer Science,* 2016, **5**, (6), pp. 17110-17115.
[40] Callavik, M., Blomberg, A., Hafner, J. and Jacobson, B.: 'The hybrid HVDC breaker: An innovation breakthrough enabling reliable HVDC grids', ABB Grid Syst., Zurich, Switzerland, Tech. Paper, Nov. 2012.
[41] Yeckley, R. and Perulfi, J.: 'Oil Circuit Breakers: A Look at the Earlier Generation [History]', *IEEE Power and Energy Magazine,* 2018, **16**, (3), pp. 86-97.
[42] Bachmann, B., Mauthe, G., Ruoss, E., Lips, H., et al: 'Development of a 500 kV airblast HVDC circuit breaker', *IEEE Transactions on Power Apparatus and Systems*, 1985, **104**, (9), pp. 2460–2466.
[43] Fontchastagner, J., Chadebec, O., Schellekens, H., and Meunier, G., et al.: 'Coupling of an electrical arc model with FEM for vacuum interrupter designs', *IEEE Transactions on Magnetics,* 2005, **41**, (5), pp. 1600-1603.
[44] Nakao, H., Nakagoshi, Y., Hatano, M., Koshizuka, T., et al: 'DC current interruption in HVDC SF6 gas MRTB by means of self-excited oscillation superimposition', *IEEE Transactions on Power Delivery*, 2001, **16**, (4), pp. 687–693.
[45] Liu, G., Xu, F. and Zhou, Y.: 'Optimized Coordinated Control Strategy of Assembly HVDC Breakers for MMC Based HVDC Grids', *Proc. 2018 International Conference on Power System Technology*, 2018, pp. 221-229
[46] Liu, L., Liu, S. and Popov, M.: 'Optimized algorithm of active injection circuit to calibrate DC circuit breaker', *International Journal of Electrical Power & Energy Systems,* 2018, **103**, pp. 369-376.
[47] Xu, B., Ding, R., Zhang, J., and Sha, L., et al.: 'Multiphysics Coupled Modeling: Simulation of Hydraulic Operating Mechanism for SF6 High Voltage Circuit Breaker', *IEEE/ASME Transactions on Mechatronics,* pp. 379-393.
[48] Liu, W., Liu, F., Zha, X., and Huang, M., et al.: 'An Improved SSCB Combining Fault Interruption and Fault Location Functions for DC Line Short Circuit Fault Protection', *IEEE Transactions on Power Delivery,* 2019, early access.
[49] L. Ängquist, A. Baudoin, T. Modeer, S. Nee and S. Norrga, 'VARC – A Cost-Effective Ultrafast DC Circuit Breaker Concept, ' *2018 IEEE Power & Energy Society General Meeting (PESGM)*, Portland, OR, 2018, pp. 1-5.
[50] S. Liu, M. Popov, S. S. Mirhosseini, S. Nee. T. Moder, L. Anquist, K. Koreman and M. van der Meijden, 'Modelling, Experimental Validation and Application of VARC HVDC Circuit Breakers, ' *IEEE Transactions on Power Delivery*, early access, 2020.
[51] Hassanpoor, A., Hafner, J. and Jacobson, B.: 'Technical Assessment of Load Commutation Switch in Hybrid HVDC Breaker', *IEEE Transactions on Power Electronics,* 2015, **30**, (10), pp. 5393-5400.
[52] Wen, W., Huang, Y., Cheng, T., and Gao, S., et al.: 'Research on a current commutation drive circuit for hybrid dc circuit breaker and its optimisation design', *IET Generation, Transmission & Distribution,* 2016, **10**, (13), pp. 3119-3126.
[53] Corea-Araujo, J. A., Martinez-Velasco, J. A. and Magnusson, J.: 'Optimum design of hybrid HVDC circuit breakers using a parallel genetic algorithm and a MATLAB-EMTP environment', *IET Generation, Transmission & Distribution,* 2017, **11**, (12), pp. 2974-2982.

[54] Wang, S., Song, Z., Fu, P., and Wang, K., et al.: 'Thermal Analysis of Water-Cooled Heat Sink for Solid-State Circuit Breaker Based on IGCTs in Parallel', *IEEE Transactions on Components, Packaging and Manufacturing Technology,* 2019, **9**, (3), pp. 483-488.
[55] Mackey, L., Peng, C. and Husain, I.: 'Progressive Switching of Hybrid DC Circuit Breakers for Faster Fault Isolation', *Proc. 2018 IEEE Energy Conversion Congress and Exposition (ECCE)*, 2018, pp. 7150 -7157.
[56] B. Yang, et al. 'A novel commutation-based hybrid HVDC circuit breaker', *CIGRÉ Winnipeg Colloquium*, Canada, Oct., 2017.
[57] Liu, W., Liu, F., Zhuang, Y., and Zha, X., et al.: 'A Multiport Circuit Breaker-Based Multiterminal DC System Fault Protection', *IEEE Journal of Emerging and Selected Topics in Power Electronics,* 2019, **7**, (1), pp. 118-127.
[58] Liu, W., Liu, F., Zha, X., and Chen, C., et al.: 'A topology of the multi-port DC circuit breaker for multi-terminal DC system fault protection', *Proc. 2017 IEEE Energy Conversion Congress and Exposition (ECCE)*, 2017, pp. 3760-3763.
[59] F. Zhang, Y. Ren, Z. Shi, X. Yang, W. Chen, 'Novel Hybrid DC Circuit Breaker Based on Series Connection of Thyristors and IGBT Half-Bridge Submodules, ' 2021, *IEEE Transactions on Power Electronics*, **36**, (2), pp. 1506-1518.
[60] J. Zhu, X. Guo, J. Yin, Q. Huo and T. Wei, 'Basic Topology, Modeling and Evaluation of a Novel Hybrid DC Breaker for HVDC Grid,' *IEEE Transactions on Power Delivery*, 2021, early access.
[61] T. Augustin, M. Becerra and H. Nee, 'Enhanced Active Resonant DC Circuit Breakers Based on Discharge Closing Switches,' in *IEEE Transactions on Power Delivery, 2021, early access.*
[62] Y. Guo, G. Wang, D. Zeng, H. Li and H. Chao, 'A Thyristor Full-Bridge-Based DC Circuit Breaker,' *IEEE Transactions on Power Electronics*, 2020, **35**, (1), pp. 1111-1123.
[63] S. Wang, C. E. Ugalde-Loo, C. Li, J. Liang and O. D. Adeuyi, 'Bridge-Type Integrated Hybrid DC Circuit Breakers,' *IEEE Journal of Emerging and Selected Topics in Power Electronics*, 2020, **8**, (2), pp. 1134-1151.
[64] J. He, Y. Luo, M. Li, Y. Zhang, *et al*., 'A High-Performance and Economical Multiport Hybrid Direct Current Circuit Breaker,' *IEEE Transactions on Industrial Electronics*, 2020, **67**, (10), pp. 8921-8930.
[65] S. Wang, W. Ming, W. Liu, C. Li, C. E. Ugalde Loo and J. Liang, 'A Multi-Function Integrated Circuit Breaker for DC Grid Applications,' *IEEE Transactions on Power Delivery, 2021, early access.*
[66] O. Cwikowski *et al*., 'Integrated HVDC circuit breakers with current flow control capability,' *IEEE Transactions on Power Delivery*, 2018, **33**, (1), pp, 371-380.
[67] E. Veilleux and B. Ooi, 'Multiterminal HVDC With Thyristor Power-Flow Controller,' in *IEEE Transactions on Power Delivery*, 2012, **27**, (3), pp. 1205-1212.
[68] Q. Mu, J. Liang, Y. Li and X. Zhou, 'Power flow control devices in DC grids,' *IEEE Power and Energy Society General Meeting*, San Diego, 2012, pp. 1-7.
[69] C. D. Barker and R. S. Whitehouse, 'A current flow controller for use in HVDC grids,' *10th IET International Conference on AC and DC Power Transmission (ACDC 2012)*, Birmingham, 2012, pp. 1-5.
[70] Stumpe, M., Tünnerhoff, P., Dave, J., and Schnettler, A., et al.: 'DC fault protection for modular multi-level converter-based HVDC multi-terminal systems with solid state circuit breakers', *IET Generation, Transmission & Distribution,* 2018, **12**, (12), pp. 3013-3020.
[71] Liu, S., Liu, Z., de Jesus Chavez, J., and Popov, M.: 'Mechanical DC circuit breaker model for real time simulations', *International Journal of Electrical Power & Energy Systems,* 2019, **107**, pp. 110-119.
[72] Mirhosseini S. S., Liu S., Muro J. C., Liu Z., Jamali S., Popov M., 'Modeling a voltage source converter assisted resonant current DC breaker for real time studies', *International Journal of Electrical Power & Energy Systems, 2020,* 117.
[73] Wang, S., Li, C., Adeuyi, O. D., and Li, G., et al.: 'Coordination of MMCs with Hybrid DC Circuit Breakers for HVDC Grid Protection', *IEEE Transactions on Power Delivery,* 2019, **34**, (1), pp. 11-22.
[74] H. Xiao, Z. Xu, L. Xiao, C. Gan, F. Xu and L. Dai, 'Components Sharing Based Integrated HVDC Circuit Breaker for Meshed HVDC Grids,' *IEEE Transactions on Power Delivery*, Aug. 2020, **35**, (4), pp. 1856-1866.
[75] C. Meyer, M. Kowal and R. W. De Doncker, 'Circuit breaker concepts for future high-power DC-applications, ' *Fourtieth IAS Annual Meeting. Conference Record of the 2005 Industry Applications Conference*, 2005, Kowloon, Hong Kong, 2005, pp. 860-866.
[76] Mitra, B., Chowdhury, B.: 'Comparative Analysis of Hybrid DC Breaker and Assembly HVDC Breaker', *Proc. North American Power Symposium*, Morgantown, WV, 2017.
[77] T. Schultz, V. Lenz and C. M. Franck, 'Circuit Breakers for Fault Current Interruption in HVDC Grids, ' *VDE High Voltage Technology 2016; ETG-Symposium*, Berlin, Deutschland, 2016, pp. 1-6.
[78] Derakhshanfar, T. U. Jonsson, U. Steiger and M. Habert, 'Hybrid HVDC breaker- A solution for future HVDC system,' *Cigre 2014*, Paris, France, 2014.
[79] M. Rahimo, et al. 'The Bimode Insulated Gate Transistor (BIGT), an ideal power semiconductor for power electronics based DC Breaker applications', *CIGRE Parsis session 2014*, pp. B4-302.
[80] VEIKAI Vacuum Interrupter VK12-40.5P, Alibaba Global Direct Sourcing Platform, https://www.alibaba.com/product-detail/VK12-40-5P-40-5KV-31_62464937198.html?spm=a2700.7724857.normalList.57.7e504b81SrdmYr
[81] F. Xu, Y. Lu, X. Ni and C. Wang, 'A Low-Cost Multi-Port Type HVDC Breaker for HVDC Grids, ' *2019 IEEE International Conference on Energy Internet (ICEI)*, Nanjing, China, 2019, pp. 121-126.
[82] S. Zhang, G. Zou, X. Wei and C. Sun, 'Diode-Bridge Multi-Port Hybrid DC Circuit Breaker for Multi-Terminal DC Grids,' *IEEE Transactions on Industrial Electronics*, early access.

[83] Ased, G. P., Li, R., Holliday, D., and Finney, S., et al: 'Continued operation of multi-terminal HVDC networks based on modular multilevel converters', *Proc. Cigré International Symposium*, 2015, pp.1-8.
[84] Yang, S., Xiang, W., Lu, X., Zuo, W., et al.: 'An adaptive reclosing strategy for MMC-HVDC systems with hybrid DC circuit breakers'. *IEEE Transactions on Power Delivery*, 2019, early access.
[85] Wang, T., Song, G. and Hussain, K.S.T., 'Adaptive Single-Pole Auto-Reclosing Scheme for Hybrid MMC-HVDC Systems breakers'. *IEEE Transactions on Power Delivery*, 2019, **34**, (6), pp. 2194-2203.
[86] Li, B., Cui, H., Li, B., Wen, W., & Dai, D. : 'A permanent fault identification method for single-pole grounding fault of overhead transmission lines in VSC-HVDC grid based on fault line voltage', *International Journal of Electrical Power & Energy Systems,* 2020, **117**, pp. 105603.
[87] Li, B., He, J., Li, Y., & Wen, W., 'A Novel DCCB Reclosing Strategy for the Flexible HVDC Grid breakers'. *IEEE Transactions on Power Delivery*, 2020, **35**, (1), pp. 244-257.
[88] Fan, X., Zhang, B. 'DC line soft reclosing sequence for HVDC grid based on hybrid DC breaker'. *The Journal of Engineering*, 2019, **16**, pp. 1095-1099.
[89] Xiangyu, P. E. I., Guangfu, T. A. N. G., & Zhang, S., 'Sequential auto-reclosing strategy for hybrid HVDC breakers in VSC-based DC grids'. *Journal of Modern Power Systems and Clean Energy*, 2019, **7,** (3), pp. 633-643.
[90] M. Cheah-Mane, O. D. Adeuyi, J. Liang and N. Jenkins, 'A scaling method for a multi-terminal DC experimental test rig', *17th European Conference on Power Electronics and Applications (EPE'15 ECCE-Europe)*, Geneva, 2015, pp. 1-9.
[91] Shemshadi A., 'Modeling of Plasma Dispersion Process in Vacuum Interrupters During Postarc Interval Based on FEM', *IEEE Transactions on Plasma* Science, 2019, **47**, (1), pp. 647-653.
[92] Li G., Liang J., Balasubramaniam S., Joseph T. and Kong D., 'Experimental validation of DC circuit-breakers for MTDC grid protection', *15th IET International Conference on AC and DC Power Transmission (ACDC 2019)*, Coventry, UK, 2019, pp. 1-6.
[93] O. N. Cwikowski, 'Synthetic Testing of High Voltage Direct Current Circuit Breakers'. PhD thesis in the University of Manchester, 2016.
[94] Liang, D., Guo, X., Gao, Y., and Zou, J., et al.: 'Investigations on A New Synthetic Test of DC Vacuum Circuit Breaker', *Proc. 2018 IEEE 3rd Advanced Information Technology, Electronic and Automation Control Conference (IAEAC)*, 2018, pp. 1376-1379.
[95] Belda, N. A., & Smeets, R. P. P., 'Test circuits for HVDC circuit breakers', *IEEE Transactions on Power Delivery*, 2017, **32**, (1), pp. 285-293.
[96] Belda, N. A., Plet, C. A., & Smeets, R. P. P., 'Full-Power Test of HVDC Circuit-Breakers with AC Short-Circuit Generators Operated at Low Power Frequency', *IEEE Transactions on Power Delivery*, 2019, **34**, (5), pp. 1843-1852.
[97] X. Han, W. Sima, M. Yang, L. Li, T. Yuan and Y. Si, 'Transient Characteristics Under Ground and Short-Circuit Faults in a MMC-Based HVDC System With Hybrid DC Circuit Breakers,' *IEEE Transactions on Power Delivery*, 2018, **33**, (3), pp. 1378-1387.

Zhou Liu (zli@et.aau.dk) received his PhD degree in energy technology at Aalborg University, Denmark in 2013. Since Dec. 2014, he started to work as a postdoc researcher at the Department of Electrical Power Engineer, Norwegian University of Science and Technology. From 2017 to 2018, he worked as a postdoc fellow at Department of Electrical Sustainable Energy, TU Delft, Netherlands. And now he is working as Assistant Professor in Department of Energy Technology, Aalborg University, Denmark. He has been involved in PROMOTioN project at TU Delft and EUDP COPE project at AAU. He is a senior member of IEEE.

Seyed Sattar Mirhosseini (s_mirhoseini@elec.iust.ac.ir) received the B.Sc. degree from the Iran University of Science and Technology (IUST), Tehran, Iran, in 2010, the M.Sc. degree from the Shahed University, Tehran, Iran, in 2013, and the Ph.D. degree from IUST, in 2021, all in electrical engineering. His research interests include power system protection in particular protection of multi-terminal HVdc grids, and HVdc circuit breakers. He has been involved in PROMOTioN project as a visiting researcher at TU Delft. He is a Student Member of the IEEE.

Lian Liu (lian.liu@prysmiangroup.com) received the B.Sc and M.Sc degrees in electrical engineering from Wuhan University, Wuhan, China, in 2010 and 2013, respectively, and the Ph.D. degree from the Department of Electrical Sustainable Energy, Delft University of Technology, Delft, The Netherlands, in 2019. His Ph.D. program was financed by China Scholarship Council. From 2017 to 2018, he was a Research Associate with the Department

of Electrical Sustainable Energy, Delft University of Technology. He has been involved in PROMOTioN project at TU Delft.

Marjan Popov (M.Popov@tudelft.nl) obtained his Ph.D. degree in electrical power engineering from the TU Delft in 2002. In 1997, he was an Academic Visitor at the University of Liverpool. His current research interests include future power systems, large-scale power system transients, intelligent protection for future power systems, and wide-area monitoring and protection. Prof. Popov is a member of CIGRE and actively participated in WG C4.502 and WG A2/C4.39. He was a recipient of the IEEE PES Prize Paper Award and the IEEE Switchgear Committee Award in 2011. He is an Associate Editor of the International Journal of Electric Power and Energy Systems. In 2017, he founded the Dutch Power System Protection Centre to promote the research and education in Intelligent Power System Protection.

Kaiqi Ma (kma@et.aau.dk) received the B.Sc. and M.Sc. degrees from Hohai University, China, in 2012 and 2015, in control engineering, respectively. He was Research Associate at Research & Development Center of State Grid Xuji Group Corporation, China. Since 2018, he has been a PhD student at the Department of Energy Technology, Aalborg University, Denmark. His research interest includes distributed generation, wind power generation, and relay protection. He is a student member of IEEE.

Weihao Hu (whu@uestc.edu.cn) is currently a Full Professor and the Director of Institute of Smart Power and Energy Systems (ISPES) at the University of Electronics Science and Technology of China (UESTC). He has led/participated in more than 15 research projects and has more than 140 publications. He has been Guest Editor of the IEEE TRANSACTIONS ON POWER SYSTEMS Special Section: Enabling very high penetration renewable energy integration into future power systems. He was serving as the Technical Program Chair (TPC) for IEEE ISGT Asia 2019. His research interests include intelligent energy systems and renewable power generation. He is a member of the IEEE Industrial Electronics Society.

Sadegh Jamali (sjamali@iust.ac.ir) received his B.Sc. from Sharif University of Technology, Iran, in 1979, M.Sc. from University of Manchester, UK, in 1986, and Ph.D. from University of London, UK, in 1990, all in electrical engineering. Professor Jamali is currently with the School of Electrical Engineering at Iran University of Science and Technology. He is a Fellow of the IET and a Chartered Engineer in the UK. His research findings have been published in over 250 papers in journals and international conferences. His research area includes power system protection, distribution systems and railway electrification where he is heavily involved in industrial consultancy.

Peter Palensky (P.Palensky@tudelft.nl) is Professor for intelligent electric power grids at TU Delft, Netherlands. Before that he was Principal Scientist for Complex Energy Systems at the Austrian Institute of Technology (AIT) / Energy Department, Austria, Head of Business Unit ”Sustainable Building Technologies” at the AIT, CTO of Envidatec Corp., Hamburg, Germany, associate Professor at the University of Pretoria, South Africa, and researcher at the Lawrence Berkeley National Laboratory, California. His works on the digital aspects of intelligent energy systems and operates an RTDS-based power system digital twin at TU Delft. He is a member of the IEEE Industrial Electronics Society.

Zhe Chen (zch@et.aau.dk) received the Ph.D. degree in electrical engineering from the University of Durham, U.K. He is a Full Professor with the Department of Energy Technology, Aalborg University, Denmark. He is the Leader of Wind Power System Research Program with the Department of Energy Technology, Aalborg University and the Danish Principle Investigator for Wind Energy of Sino-Danish Centre for Education and Research. His main current research interests are power electronics, power grids and new energy technologies. He has led and participated in many research and industrial projects and has been a panel member of research funding evaluation committees in many EU countries. He is a Fellow of the IET and IEEE, and a Chartered Engineer in the UK. He is a member of the IEEE Industrial Electronics Society.